ChemBioChem

Research Article
doi.org/10.1002/cbic.202200040

Chemistry Europe
European Chemical Societies Publishing

www.chembiochem.org

VIP *Very Important Paper*

Isolation of Tobacco Mosaic Virus-Binding Peptides for Biotechnology Applications

Soo Khim Chan[b] and Nicole F. Steinmetz*[a]

Tobacco mosaic virus (TMV) was the first virus to be discovered and it is now widely used as a tool for biological research and biotechnology applications. TMV particles can be decorated with functional molecules by genetic engineering or bioconjugation. However, this can destabilize the nanoparticles, and/or multiple rounds of modification may be necessary, reducing product yields and preventing the display of certain cargo molecules. To overcome these challenges, we used phage display technology and biopanning to isolate a TMV-binding peptide (TBP_{T25}) with strong binding properties (IC_{50} = 0.73 μM, K_D = 0.16 μM), allowing the display of model cargos via a single mixing step. The TMV-binding peptide is specific for TMV but does not recognize free coat proteins and can therefore be used to decorate intact TMV or detect intact TMV particles in crude plant sap.

Introduction

Tobacco mosaic virus (TMV) is a well-characterized plant virus that forms rigid nanotube-like particles with dimensions of 300×18 nm. This hollow nanotube comprises 2130 identical copies of the ~18-kDa TMV coat protein, forming a helical capsid around the ~6400-nt single-stranded RNA genome.[1] The TMV coat protein (CP) is a ring that has a dimer of bilayer disks with 17 subunits per layer.[2] The subunit is held by four main α-helices bundle[3] with both N- and C-terminus exposed on the surface of CP.[4] TMV infects more than 350 plant species and causes significant crop losses,[5] but it is also a prominent model virus for biological research and has several biotechnological applications. For example, TMV has been functionalized by displaying various molecules on its surface, and the modified viral nanoparticles (VNPs) have been integrated into electronic devices, used as immobilized catalysts, and developed for numerous biomedical purposes.[6]

The functionalization of TMV can be achieved by genetic engineering or bioconjugation.[7,8] In a recent example, TMV was used for the multivalent display of SARS-CoV-2 antigens and its efficacy as a COVID-19 vaccine candidate was demonstrated in mice.[9] In this case, bioconjugation was used to attach the antigens to the TMV particles. In another example, TMV was developed as an adjuvant by non-specifically absorbing antigens to its surface, resulting in a potent immune response.[10] The latter method avoids the need for a multi-step conjugation process but is limited to cargo molecules with surface chemistry that can induce non-specific binding, and the resulting particles may be unstable *in vivo* or in storage. We therefore need additional innovative display technologies for TMV, combining simplicity with particle stability.

To address this challenge, we considered the potential of biospecific functionalization based on TMV-binding peptides (TBPs). Peptides that bind strongly and specifically to TMV could be synthesized and attached to a variety of functional molecules, and then mixed with native TMV particles to achieve cargo display by single-step high-affinity binding. We recently demonstrated the potential of this approach for another plant virus, cowpea mosaic virus (CPMV). We isolated CPMV-specific peptides by combining phage display with biopanning, and we demonstrated that CPMV could be functionalized with various medically relevant cargos for delivery to cancer cells.[11] Others have used a structure-based approach to define CPMV-binding peptides for the development of biosensors and diagnostics.[12]

To the best of our knowledge, TMV-specific peptides have not been reported thus far. Accordingly, we modified our phage display and biopanning approach to screen for TBPs.[13] After four rounds of biopanning using a commercially available 12-mer M13-based phage library, we identified GHRCRGGVCYKK as a high-affinity TBP. The peptide was functionalized with model cargo molecules and tested for its ability to display them on TMV and other plant viruses. As proof of principle for diagnostics applications, we also tested the ability of the TBPs to detect TMV in crude plant sap.

Results and Discussion

Production and characterization of TMV

TMV was propagated in and purified from *Nicotiana benthamiana* leaves as previously described.[14] Purified TMV particles were then characterized by sodium dodecylsulfate polyacryla-

[a] *Prof. Dr. N. F. Steinmetz*
Department of NanoEngineering
Department of Bioengineering, Department of Radiology
Center for Nano-ImmunoEngineering, Moores Cancer Center
Institute for Materials Discovery and Design
University of California San Diego
9500 Gilman Dr., La Jolla CA 92093 (USA)
E-mail: nsteinmetz@ucsd.edu
[b] *Dr. S. K. Chan*
Department of Nanoengineering
University of California San Diego
9500 Gilman Dr., La Jolla CA 92093 (USA)

Supporting information for this article is available on the WWW under https://doi.org/10.1002/cbic.202200040

mide gel electrophoresis (SDS-PAGE), ultraviolet-visible (UV-Vis) spectrophotometry, transmission electron microscopy (TEM), size exclusion chromatography (SEC), and dynamic light scattering (DLS). Denaturing SDS-PAGE revealed the presence of a single ~18-kDa band representing the TMV coat protein (Figure 1A). The 260/280 absorbance ratio of ~1.2 indicated the absence of contaminants (Figure 1B).[15] TEM showed the presence of intact 300 nm sized TMV nanotubes (Figure 1C). However, longer or shorter TMV nanorods are also observed by TEM imaging (Figure S1) due to end-to-end assembly[16] or fragmented particles due to handling during TEM sample preparation[17] The purity of the particles was confirmed by SEC, yielding a single elution peak at ~10 mL from a Superose 6 column, with no free RNA (260 nm) or protein (280 nm) detected (Figure 1D). Finally, DLS indicated a polydispersity index (PDI) of 0.187 and diameter of ~146 nm, as reported previously for TMV,[18] further confirming the monodispersity of the particles (Figure 1E).

Isolation of TMV-binding monoclonal phages

We used a commercial PhD-12 Phage Display Peptide Library Kit consisting of 10^{13} pfu/mL M13 phage to isolate candidate TBPs. The input library was pre-incubated overnight to remove peptides that bind to bovine serum albumin (BSA) before exposure to TMV. Four rounds of selection (biopanning) were carried out to enrich for TBPs by increasing the washing stringency (0.1%, 0.3%, 0.4% and 0.5% (v/v) Tween-20), thus removing non-specific and weak binders. The enrichment of TMV-binding monoclonal phages was confirmed in a polyclonal enzyme-linked immunosorbent assay (ELISA; Figure 2A) and a plaque titer assay (Table S1). We achieved five-fold enrichment by the end of fourth cycle, and 40 monoclonal phages were selected randomly from the enriched phage pool for monoclonal ELISA against TMV and BSA as a negative control (Figure 2B). Among the 40 candidates, only monoclonal phage T25 bound to TMV, resulting in a differential absorbance of 0.3 units compared to BSA. T25 was therefore selected for DNA sequencing. Some nonspecific binding to BSA was observed, resulting in a slightly higher BSA signal (~0.26) compared to the other phages (~0.10).

The motif displayed on phage T25 was GHRCRGGVCYKK. To determine its specificity for TMV, we exposed monoclonal phage T25 to TMV as well as various other plant viruses, specifically CPMV, cowpea chlorotic mottle virus (CCMV), potato virus X (PVX), and tobacco mild green mosaic virus (TMGMV). We also exposed it to virus-like particles (VLPs) based on bacteriophage Qβ and physalis mottle virus (PhMV), as well as BSA as a negative control. The characterization of the non-target viruses and VLPs is described in our previous work.[8] The binding of phage T25 to TMV and non-target viruses/VLPs was compared by ELISA (Figure 2C), with empty M13 phage (M13KE) used to rule out false-positive binding. Monoclonal phage T25 bound with the highest affinity to TMV, but some background binding was observed for TMGMV and CPMV (1.2-fold less than TMV). TMGMV shares 64% sequence identity with TMV so some cross-reaction was anticipated.[19] However, given the absence of homology between TMV and CPMV, the binding of TBP to CMPV is more likely to reflect off-target binding. There was no

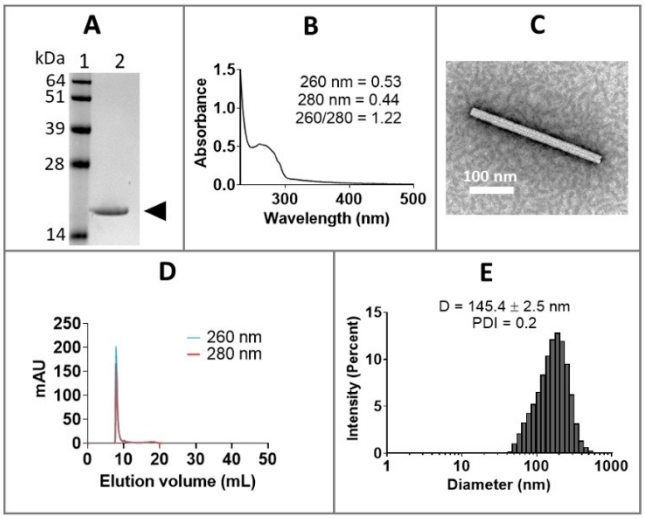

Figure 1. Characterization of TMV. (A) Denaturing SDS-PAGE. Lane 1 = SeeBlue Plus2 Pre-stained Protein Standard; Lane 2 = TMV, with the arrow indicating the coat protein band at ~18 kDa. (B) UV-Vis spectrum showing absorbance at 260 and 280 nm, resulting in a 260/280 ratio of ~1.2 as expected for pure TMV. (C) Negatively stained TMV imaged by TEM. (D) TMV SEC profiles following elution from a Superose 6 column. Nucleic acids were detected at 260 nm, and protein was detected at 280 nm. (E) Representative data following the analysis of triplicate TMV samples by DLS (D = average particle diameter, PDI = polydispersity index). Average particle diameter was tabulated from the mean intensity of three separate runs.

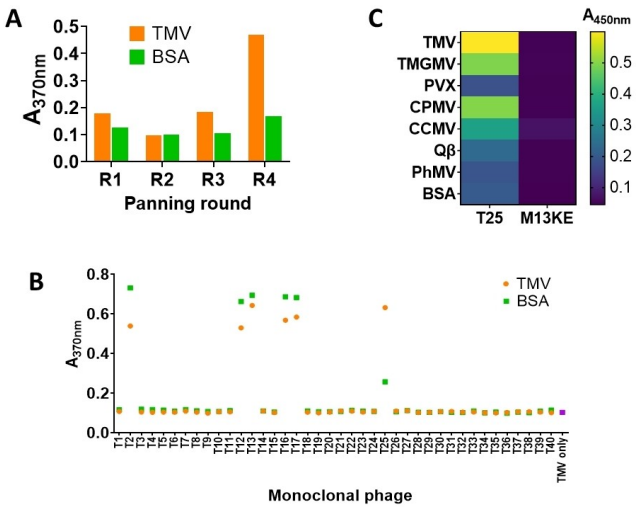

Figure 2. Isolation and validation of TMV-binding monoclonal phages. (A) Polyclonal ELISA of enriched binders from each round against TMV. (B) Monoclonal ELISA of 40 monoclonal phages against TMV (orange dots) and BSA (green dots). TMV only (purple dot) served as a negative control. (C) Heatmap showing cross-reactivity of monoclonal phage T25 and M13KE (empty phage) against TMV and other viruses/VLPs. TMV = tobacco mosaic virus, TMGMV = tobacco mild green mosaic virus, PVX = potato virus X, CPMV = cowpea mosaic virus, CCMV = cowpea chlorotic mottle virus, Qβ = bacteriophage Qβ VLP, PhMV = Physalis mottle virus VLP, BSA = bovine serum albumin (negative control).

cross-reactivity between M13KE and the other viruses or VLPs. Furthermore, none of the viruses or VLPs bound to M13KE, confirming that the ability of phage T25 to bind TMV was indeed conferred by the displayed TBP.

Characterization of the synthetic peptide TBP_{T25}

The sequence of the TMV-binding peptide from phage T25 (TBP_{T25}) was screened using the online tool Scanner and Reporter of Target-Unrelated Peptides (SAROTUP) and was predicted neither to bind polystyrene (probability <0.1) nor to contain motifs unrelated to the target (Table S2). TBP_{T25} was therefore synthesized with separate biotin and fluorescein isothiocyanate (FITC) modifications at the C-terminus for further testing. The C-terminus was selected for labeling because this was the end linked to the phage and is therefore unlikely to be required for TMV binding. TBP_{T25}-biotin was used to detect assembled TMV particles and free TMV coat proteins. Characterization of TMV coat proteins is shown in Figure S2. TMV coat protein is smaller in size compared to full-length TMV and has lower RNA/protein content (indicated by lower 260/280 ratio). Western blots of the coat proteins separated by denaturing SDS-PAGE revealed no binding to the TBP_{T25}-biotin probe (data not shown). For confirmation, we spotted free coat protein and assembled TMV particles onto a nitrocellulose membrane under native conditions. The TBP_{T25}-biotin probe bound to the intact particles but not to the free coat protein (Figure 3A), indicating that TBP_{T25} recognizes a conformational epitope only present in the assembled particles. Binding of TBP_{T25}-biotin to TMV was also demonstrated by immunogold-labeling and TEM imaging (Figure 3B). This finding was validated by ELISA, following the immobilization of TBP_{T25}-biotin on streptavidin plates followed by the addition of TMV particles (Figure 3C). ELISA indicates binding of TMV to the TBP_{T25}-biotin coated plates while low signals were observed for the controls 1 and 2 in Figure 3C (Control 1 = TBP_{T25}-biotin omitted and Control 2 = TMV omitted). Similar observations were made when TMV was probed against random peptides: TMV binding to the TMV-specific TBP_{T25} was confirmed, but TMV did not bind to a CPMV-specific biotinylated peptide (CBP-Biotin) that we isolated in previous work[8] (Figure S3). Similarly, TBP_{T25}-FITC probes were shown to bind to TMV more significantly than to BSA (Figure S4), and concentration dependence was noted: the more TMV coated onto the plates, the higher signal for TBP_{T25}-FITC (Figure S5). Moreover, while there was some background binding to BSA, peptides pre-blocked with BSA continued to exhibit significant binding to TMV (Figure S6). Together these data provide convincing evidence that the TBP_{T25} binds to intact TMV particles.

Competitive ELISA was then used to determine the K_D and IC_{50} values of TBP_{T25}-biotin (Figure 3D). Monoclonal phage T25 and TBP_{T25}-biotin (0.5–0 μg) were incubated together to compete for the same binding site on TMV. A horseradish peroxidase (HRP)-conjugated anti-M13 monoclonal antibody was used to detect the bound monoclonal phage T25. The quantity of bound monoclonal phage T25 reduced with increasing amounts of TBP_{T25}-biotin to yield values of IC_{50} = 0.73 μM and K_D = 0.16 μM.

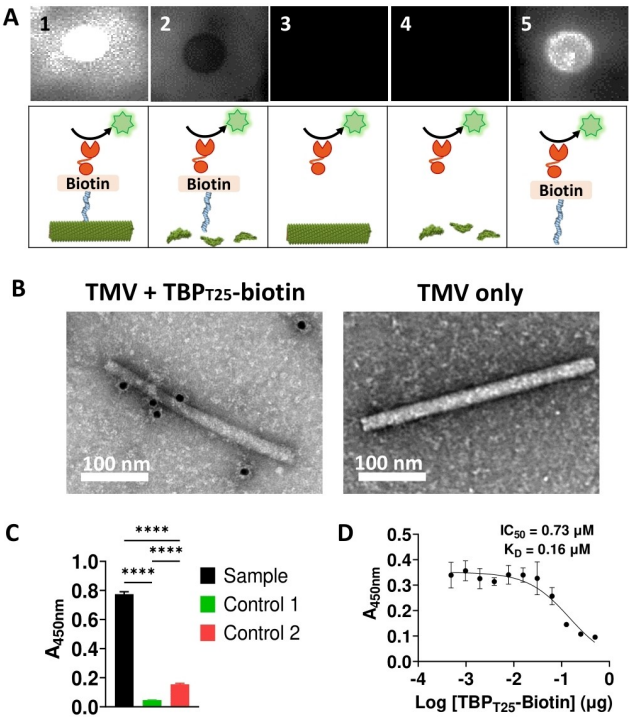

Figure 3. (A) Dot blot to investigate the binding of TBP_{T25}-biotin to TMV particles and coat proteins (CPs). (1) TMV probed with TMV_{T25}-biotin. (2) TMV CPs probed with TMV_{T25}-biotin. (3) TMV only (negative control). (4) TMV CPs only (negative control). (5) TBP_{T25}-biotin only (positive control). (B) Immunogold-labeling and TEM imaging. TMV-TBP_{T25}-biotin complex (sample) and TMV only without TBP_{T25}-biotin (control) were treated with a goat anti-biotin antibody (10 nm-sized gold label) and stained with 2% (w/v) UAc. (C) Analysis of TBP_{T25}-biotin by ELISA. Sample = TBP_{T25}-biotin coated onto streptavidin plates followed by incubation with TMV; detection was carried out with anti-TMV rabbit polyclonal antibodies followed by HRP-conjugated goat anti-rabbit antibody. Control 1 = TBP_{T25}-biotin omitted. Control 2 = TMV omitted. Results were compared by one-way ANOVA (****$p<0.0001$). (D) Competitive ELISA between TBP_{T25}-biotin and monoclonal phage T25. The half maximal inhibitory concentration (IC_{50}) was determined by nonlinear regression analysis (one site-fit log IC_{50}). Data are means ± standard deviations (n = 3).

TBP can be used to detect TMV in plant sap

To investigate the potential applications of TBP_{T25}, we used TBP_{T25}-biotin to detect TMV in crude plant sap. We first confirmed the presence of TMV in sap from TMV-infected leaves using a validated double antibody sandwich (DAS)-ELISA as part of a commercial detection kit (Nano Diagnostics). Briefly, plates were coated with polyclonal rabbit anti-TMV antibodies before exposure to pure TMV, sap from infected plants, or sap from healthy plants (Figure 4A). The signal was highest for pure TMV and sap from the infected leaves, whereas the signal from non-infected leaves was similar to that of the negative control in which the capture antibodies were replaced with BSA. We then repeated the assay but replaced the capture antibodies with TBP_{T25}-biotin. Again, a strong signal was observed for pure TMV

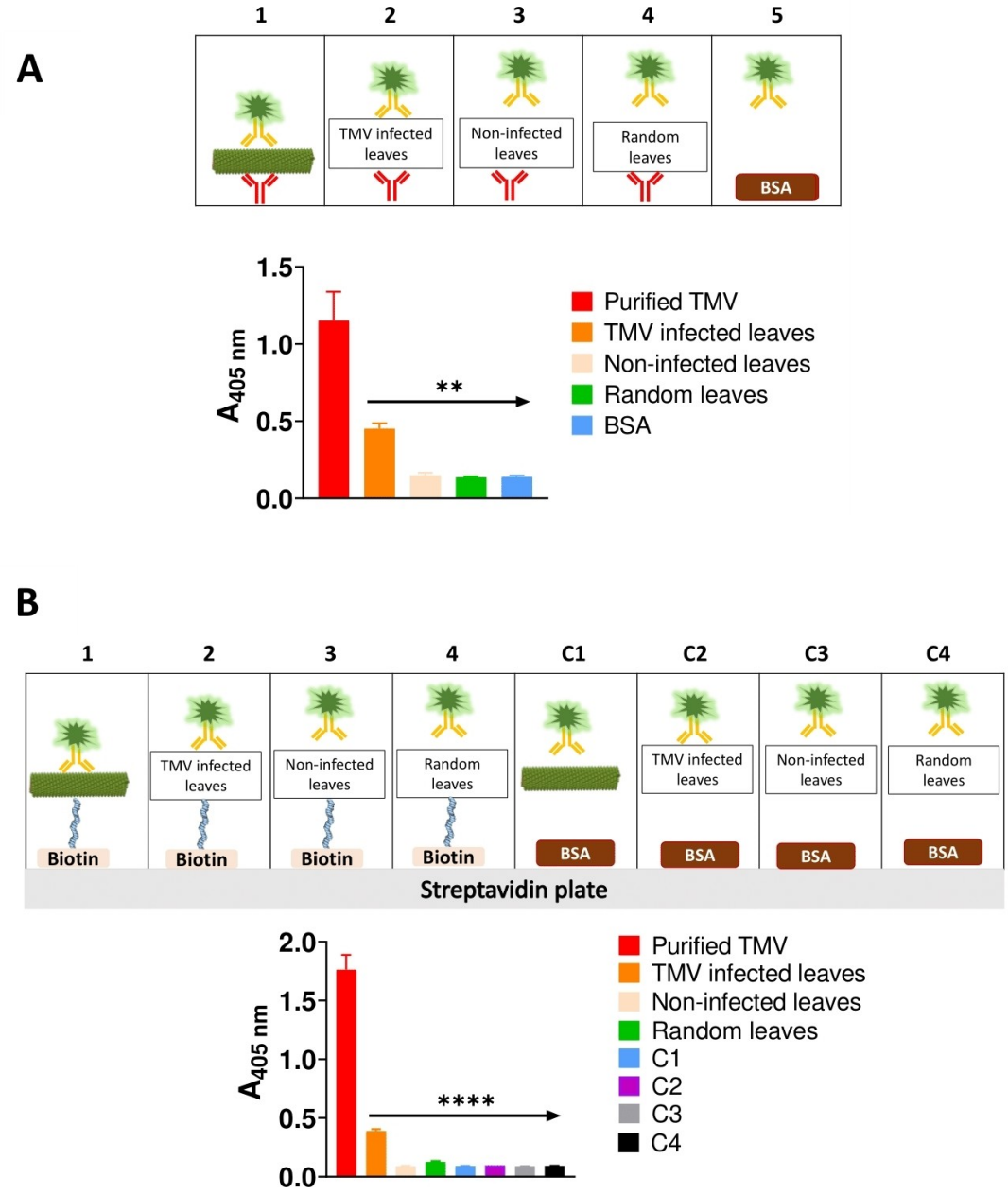

Figure 4. The ability of TBP_{T25}-biotin to capture TMV from plant sap was confirmed by ELISA. (A) Detection of TMV in plant sap using commercially available anti-TMV antibodies. Wells coated with the antibodies were incubated with (1) pure TMV, (2) sap from TMV-infected *N. benthamiana* leaves, (3) non-infected leaves, (4) random leaves, and (5) BSA as a negative control. Binding was detected using alkaline phosphatase (AP)-conjugated anti-TMV antibodies. (B) Detection of TMV in plant sap using TBP_{T25}-biotin. Wells coated with the peptide were incubated with the components described in panel (A) and we observed similar results. The control wells (C1-C4) were coated with BSA instead of TBP_{T25}-biotin. Results were compared by one-way ANOVA. Data are means ± standard deviations (n = 3). Results were compared by one-way ANOVA (**$p < 0.01$, ****$p < 0.0001$).

and the infected leaves, but the signal for healthy plants was similar to that of the BSA negative controls lacking the capture peptide (Figure 4B). These data confirm that TBP_{T25}-biotin recognizes and binds to TMV even in complex media such as plant sap, highlighting its suitability for use in diagnostic assays.

Conclusion

We isolated a TMV-binding peptide (TBP_{T25}) through four rounds of biopanning using an M13 12-mer library. Competition binding assays probing TMV with phage T25 *vs.* TBP_{T25} indicated that TBP_{T25} has an IC_{50} of 0.73 μM and a K_D of 0.16 μM. Biotin-tagged TBP_{T25}-biotin could be used to detect TMV in crude plants – as an alternative to detection with more costly antibodies. Some off-target binding to CPMV, TMGMV, and the

blocking agent BSA was observed for TBP_{T25}. Therefore, in the future, computer modeling and mutagenesis could be used to improve peptide specificity.[20] Nevertheless, TBP_{T25} functionalized with biotin or FITC recognized and bound TMV even in complex media such as plant sap (and in the presence of the blocking agent BSA). It is notable that TBP_{T25} recognizes and binds intact TMV particles but not the coat protein itself, which provides a means to distinguish between intact and disassembled particles in diagnostic assays. Other applications would include the use of TBP_{T25} for virus functionalization with antigens, therapeutic payloads, and contrast agents among others, by means of coupling these agents to the C-terminus of TBP_{T25}. Finally, given the ability of TBP_{T25} to capture TMV from complex media, it may be suitable for the development of hybrid materials, such as TMV-coated electrodes[21] or storage devices,[22] with diverse research applications.

Experimental Section

Preparation and characterization of TMV particles: TMV was produced under a USDA-approved PPQ526 permit and was purified as previously described.[14] The concentration of purified TMV was determined by UV-Vis spectrophotometry at 260 nm with an extinction coefficient (ε_{260nm}) of 3 $mg^{-1}\,mL\,cm^{-1}$. TMV preparations were characterized by TEM, DLS and SEC as previously reported.[23]

Isolation of TMV-binding peptides by biopanning: TBPs were isolated using a PhD-12 Phage Display Peptide Library Kit (New England Biolabs) as described previously with slight modifications.[8] We coated each well of a Nunc Maxisorp flat-bottom 96-well plate with 10 μg TMV and incubated plates overnight at 4 °C. Four rounds of affinity selection were carried out to enrich for TBPs by increasing the stringency of selection in each round. This was achieved by increasing the concentration of Tween-20 in TBST from 0.1% to 0.3%, 0.4% and then 0.5%. The enriched phages were eluted and amplified according to the manufacturer's protocol.

Disassembly of TMV to obtain free TMV coat proteins: Wild type (WT) TMV was disassembled to obtain free coat proteins (CPs) following an established protocol.[24] In brief, 10 mg of TMV was treated with 2 volumes of glacial acetic acid for 20 min on ice, followed by centrifugation at 20,000 *g* at 4 °C for 20 min to remove the precipitated RNAs. The supernatant was dialyzed against water for 48 h at 4 °C to obtain a white precipitate which represents the disassembled CPs. The solution was then centrifuged at 20,000 *g* at 4 °C for 20 min to obtain the CP pellet. The pellet was resuspended with 10 mM sodium phosphate buffer (pH 7.2) overnight. The concentration of CPs was determined at A260 with extinction coefficient at 1.3 $\mu L\,\mu g^{-1}\,cm^{-1}$. CPs free from RNA contamination have an absorbance ratio of A260/A280 = 0.65 and A280/A250 = 2.

ELISA

Polyclonal ELISA: We coated each well of a Nunc Maxisorp flat-bottom 96-well plate with 10 μg TMV (in 0.1 M bicarbonate buffer, pH 8.6) and incubated overnight at 4 °C. Plates coated with 5% (w/v) BSA was used as negative controls. Next day, plates were blocked with 5% (w/v) BSA and incubated at room temperature for 1 h, shaking at 800 rpm. The plates were then washed with 0.1% TBST (3×1 min). We added 20 μL of amplified phage from each biopanning cycle to each well in 5% (w/v) BSA and incubated at room temperature for 1 h, shaking at 800 rpm. Plates were then washed with 0.5% TBST (3×5 min) followed by the addition of 100 μL HRP-conjugated anti-M13 monoclonal antibody (Abcam ab50370, diluted 1:500) and incubation at room temperature for 1 h, shaking at 800 rpm. After further washes in 0.5% TBST (3×5 min) we added 100 μL of the tetramethylbenzidine (TMB) substrate (Thermo Fisher Scientific) to each well. The plates were incubated in the dark for 10 min and the absorbance was measured at 370 nm using an Infinite 200 Rx plate reader (Tecan Life Sciences) with 25 flashes in 96-well flat-bottom plate mode.

Monoclonal ELISA: The monoclonal ELISA protocol was similar to the polyclonal ELISA but we added 100 μL of amplified phage from the previous biopanning cycle to each well, followed by incubation at room temperature for 1 h, shaking at 800 rpm. Monoclonal phages differing in absorbance between TMV and BSA by at least 0.3 units were isolated for DNA sequencing (Eurofins Genomics).

Cross-reactivity assay: The cross-reactivity protocol was similar to the polyclonal ELISA but we added 10 μg of viruses or VNPs to the plates and added 10^9 pfu of phage to each well to assess their binding activity.

Synthesis and testing of TBP_{T25}: TBP_{T25}-biotin (H2 N-GHRCRGGVC YKKKGGGSK/biotin/-CO2H) and TBP_{T25}-FITC (H2 N-GHRCRGGV CYKKKGGGSK/FITC/-CO2H) were synthesized by solid phase peptide synthesis as linear peptides by GenScript with a purity of 75%. HPLC and mass spectra of peptides are available in Supporting Information as Figure S8 and Figure S9. Peptide sequence H2 N-GHRCRG GVCYKK-CO2H was obtained from monoclonal phage T25. Linker GGGS was added to C-terminus of peptide for flexibility. Additional lysine (K) was added to the end of the peptide sequence to provide side chain for modifications (FITC or biotin) via amide bond. FITC was added to side chain of lysine via addition reaction while biotin was added through substitution reaction.

Dot blots: We coated an Amersham Protran 0.45 nitrocellulose membrane (GE Healthcare) with 10 μg TMV followed by air-drying under a hood for 10 min. 2 μg of TBP_{T25}-biotin was coated directly onto the membrane to serve as positive control. The membrane was blocked with 5% (w/v) BSA for 1 h at room temperature followed washing with 0.1% TBST (3×1 min). We then added 10 μg/mL of TBP_{T25}-biotin in 5% (w/v) BSA to the membrane followed by incubation at room temperature for 1 h, shaking at 800 rpm. After washing the membranes in 0.5% TBST (3×5 min) we added the streptavidin HRP conjugate (Abcam ab7403, diluted 1:10,000 in 2% (w/v) BSA) and incubated at room temperature for 1 h, shaking at 800 rpm. The membrane was then washed with 0.5% TBST before incubation with 1 mL Pierce ECL western blotting substrate for 1 min and exposure to chemiluminescence mode for 40 s in the FluorChem R system (ProteinSimple).

ELISA: For TMV-TBP_{T25}-biotin ELISAs, we added 0.1 μg TBP_{T25}-biotin to Pierce streptavidin-coated 96-well immunoassay plates (Thermo Fisher Scientific) and incubated at room temperature for 1 h, shaking at 800 rpm. We added 5% BSA without TBP_{T25}-biotin to the control wells. Plates were blocked with 5% (w/v)

BSA followed by one wash with 0.1% TBST for 5 min. We then added 10 μg TMV and incubated at room temperature for 1 h, shaking at 800 rpm. After washing with 0.5% TBST (3×5 min) we added 100 μL anti-TMV rabbit polyclonal antibodies (diluted 1:1000) and incubated at room temperature for 1 h, shaking at 800 rpm. After washing again as above, we added 100 μL of the HRP-conjugated goat anti-rabbit antibody (Pacific Immunology, diluted 1:10,000) and incubated at room temperature for 1 h, shaking at 800 rpm. After final washes as above, we added 100 μL TMB substrate to each well and incubated the plates in the dark for 5–10 min, before stopping the reaction with 50 μL 2 M H_2SO_4. Absorbance was measured at 450 nm using an Infinite 200 Rx plate reader as described above.

For TMV-TBP_{T25}-FITC ELISAs, we coated Corning Costar 96-well white solid plates with 100 μg TMV and incubated at room temperature for 1 h, shaking at 800 rpm. Uncoated wells were used as negative controls. The plates were blocked with 5% (w/v) BSA followed by washing with 0.1% TBST (3×1 min). We then added 0.01 μg TBP_{T25}-FITC in 5% (w/v) BSA for binding and incubated at room temperature for 1 h, shaking at 800 rpm. After washing in 0.5% TBST (3×5 min), we added 100 μL distilled water to each well and measured the fluorescence using an Infinite 200 Rx plate reader with excitation and emission wavelengths of 496 nm and 519 nm, respectively.

BSA inhibition assay: Sample wells were coated with 10 μg of TMV and the control wells were coated with only 1× TBS. The plate was incubated at room temperature for 1 h with shaking at 400 rpm. The plate was later blocked with 5% (w/v) BSA for 1 h with shacking at 400 rpm. At the meantime, 0.01 μg of TBP_{T25}-biotin was incubated with a serial percentage of BSA (0, 0.5, 1, 2, 3, 4, 5, 6, 7, 8, 9, 10) for 1 h with shaking at 450 rpm. The plate was washed once with 0.1% TBST for 5 min followed by adding in the pre-blocked TBP_{T25}-biotin. The plate was incubated for 1 h with shaking at 400 rpm. After washing thrice with 0.1% TBST (5 min each time), streptavidin HRP conjugate (Abcam ab7403, diluted 1:10,000 in 5% (w/v) BSA) was added and incubated at room temperature for 1 h, shaking at 400 rpm. After further washes in 0.1% TBST (3×5 min) we added 100 μL of the tetramethylbenzidine (TMB) substrate (Thermo Fisher Scientific) to each well. The plate was incubated in the dark for ~10 min and the absorbance was measured at 450 nm using an Infinite 200 Rx plate reader (Tecan Life Sciences) with 25 flashes in 96-well flat-bottom plate mode. Equation [inhibitor] vs [response] from GraphPad Prism was used to calculate the IC_{50} of the BSA inhibition. Paired t-test was used to compute the significance difference of the two observations.

Competitive ELISA: The competitive ELISA protocol was similar to the polyclonal ELISA but with modifications to obtain the K_D and IC_{50} values. Serially diluted TBP_{T25}-biotin (0.500 μg, 0.250 μg, 0.125 μg, 0.063 μg, 0.031 μg, 0.016 μg, 0.008 μg, 0.004 μg, 0.002 μg, 0.001 μg and 0.5 ng) was added to the wells together with 6×10^9 pfu of monoclonal phage T25. The reaction after incubation with TMB substrate was stopped using 50 μL 2 M H_2SO_4. The colorimetric signal was detected at 450 nm using an Infinite 200 Rx plate reader as described above. The calculation of IC_{50} is done by GraphPad Prism using One site-Fit logIC50. This model determines the equilibrium dissociation constant of an unlabelled ligand by measuring its competition for radioligand binding. The model of this equation is Y = Bottom + (Top-Bottom)/(1 + 10(X-LogIC50)) where the top and bottom are the plateaus in the units of Y-axis. To calculate K_D, equation one-site specific binding was used where model $Y = B_{max}*X/(K_D + X)$) with Y = specific binding in A_{450nm}, X = amount of TBP_{T25}-biotin plotted in logarithm scale, and B_{max} = maximum binding from Y-axis. This equation is used to measure binding of peptide to TMV indirectly by measuring the bound monoclonal phage T25.

TEM Immunogold binding: 20 μL of TMV-TBP_{T25}-biotin was place on Formvar/carbon-coated 400 mesh copper grids (Electron Microscopy Science) for 30 min. The grid was washed once with 10 mM KP buffer (pH 7), and blocked with 1% (w/v) BSA with 0.1% (v/v) Tween-20 for 30 min followed by equilibration in 0.1% (w/v) BSA for 5 min. The grid was then placed onto a droplet of goat anti-biotin (1:5 dilution, 10 nm-sized gold labels, Aurion) and incubated for 1 h. Following the incubation, the grid was washed once with PBST (PBS containing 0.1% (v/v) Tween-20) for 3 mins, then washed thrice with distilled water (5 min each wash). Lastly, the grid was stained with 2% (w/v) uranyl acetate (Fisher Scientific) for 2 min. Excess solution was blotted with filter paper. The grid was imaged with a JOEL 1400 transmission microscope at 80 kV.

TMV detection in plant sap using TBP as the capture agent: Plant sap was obtained from TMV-infected *N. benthamiana* leaves, healthy *N. benthamiana* leaves, and 'random leaves', specifically bougainvillea leaves collected from the street. Leaves were pulverized to fine powder under liquid nitrogen using a mortar and pestle, and 100 μg was transferred to a microcentrifuge tube and suspended in 1 mL Millipore water. The mixture was vortexed for 30 s and centrifuged at 13,000 *g* for 10 min to obtain the supernatant for analysis using a TMV-DAS ELISA kit (Nano Diagnostics, V088). We used 50 μL of plant sap with 5% (w/v) BSA for each experiment, according to the manufacturer's protocol. Parallel experiments were carried out by replacing the TMV antibody with 5 μg TBP_{T25}-biotin.

Data availability

Data available upon request from the authors.

Acknowledgements

This work was funded in part by NIH grants R21-AI161306 and R01-CA202814, by NSF through the UC San Diego Materials Research Science and Engineering Center (UCSD MRSEC; DMR-2011924), as well as a UC San Diego Galvanizing Engineering in Medicine (GEM) Award.

Conflict of Interest

Dr. Steinmetz is a co-founder of, has equity in, and has a financial interest with Mosaic ImmunoEngineering Inc. Dr.

Steinmetz serves as Director, Board Member, and Acting Chief Scientific Officer, and paid consultant to Mosaic. Dr. Chan declares no competing financial interests.

Data Availability Statement

The data that support the findings of this study are available from the corresponding author upon reasonable request.

Keywords: noncovalent display · peptides• biopanning · phage display · tobacco mosaic virus

[1] K. C. He, *Flexibility in Tobacco Mosaic Virus, in Ciba Foundation Symposium 93: Mobility and Function in Proteins and Nucleic Acids*, Vol. 93, Wiley, **2008**, pp. 116–138.
[2] X. Li, B. Song, X. Chen, Z. Wang, M. Zeng, D. Yu, D. Hu, Z. Chen, L. Jin, S. Yang, C. Yang, B. Chen, *PLoS One* **2013**, *8*, e77717.
[3] V. V. Makarov, E. V. Skurat, P. I. Semenyuk, D. A. Abashkin, N. O. Kalinina, A. M. Arutyunyan, A. G. Solovyev, E. N. Dobrov, *PLoS One* **2013**, *8*, e60942.
[4] K. Namba, R. Pattanayek, G. Stubbs, *J. Mol. Biol.* **1989**, *208*, 307–325.
[5] J. Peng, K. Song, H. Zhu, W. Kong, F. Liu, T. Shen, Y. He, *Sci. Rep.* **2017**, *7*, 1–9.
[6] G. P. Lomonossoff, C. Wege, *Adv. Virus Res.* **2018**, *102*, 149–176.
[7] A. A. Mansour, S. Banik, R. V. Suresh, H. Kaur, M. Malik, A. A. McCormick, C. S. Bakshi, *Front. Microbiol.* **2018**, *9*, 1195.
[8] J. Röder, R. Fischer, U. Commandeur, *Front. Plant Sci.* **2017**, *8*, 1125.
[9] J. M. Royal, C. A. Simpson, A. A. McCormick, A. Phillips, S. Hume, J. Morton, J. Shepherd, Y. Oh, K. Swope, J. L. DeBeauchamp, R. J. Webby, R. W. Cross, V. Borisevich, T. W. Geisbert, J. K. Demarco, B. Bratcher, H. Haydon, G. P. Pogue, *Vaccine* **2021**, *9*, 1347.
[10] E. A. Evtushenko, E. M. Ryabchevskaya, N. A. Nikitin, J. G. Atabekov, O. V. Karpova, *Sci. Rep.* **2020**, *10*, 10365.
[11] S. K. Chan, N. F. Steinmetz, *Biomacromolecules* **2021**, *22*, 3613–3623.
[12] H. Peyret, E. Groppelli, D. Clark, N. Eckersley, T. Planche, J. Ma, G. P. Lomonossoff, *J. Virol. Methods* **2022**, *300*, 114372.
[13] G. P. Smith, *Science* **1985**, *228*, 1315–1317.
[14] M. A. Bruckman, N. F. Steinmetz, *Methods Mol. Biol.* **2014**, *1108*, 173–185.
[15] R. D. Lin, N. F. Steinmetz, *Nanoscale* **2018**, *10*, 16307.
[16] S. Asurmendi, R. H. Berg, T. J. Smith, M. Bendahmane, R. N. Beachy, *Virology* **2007**, *366*, 98–106.
[17] R. D. Lin, N. F. Steinmetz, *Nanoscale* **2018**, *10*, 16307–16313.
[18] K. L. Lee, L. C. Hubbard, S. Hern, I. Yildiz, M. Gratzl, N. F. Steinmetz, *Biomater. Sci.* **2013**, *1*, 581–588.
[19] I. Solis, F. Garcia-Arenal, *Virology* **1990**, *177*, 553–558.
[20] V. D. Sood, D. Baker, *J. Mol. Biol.* **2006**, *357*, 917–27.
[21] K. Gerasopoulos, M. Mccarthy, E. Royston, J. N. Culver, R. Ghodssi, *J. Micromech. Microeng.* **2008**, *18*, 104003.
[22] R. J. Tseng, C. Tsai, L. Ma, J. Ouyang, C. S. Ozkan, Y. Yang, *Nat. Nanotechnol.* **2006**, *11*, 72–77.
[23] S. K. Chan, P. Du, C. Ignacio, S. Mehta, I. G. Newton, N. F. Steinmetz, *ACS Nano* **2020**, *15*, 1259–1272.
[24] P. Lam, N. M. Gulati, P. L. Stewart, R. A. Keri, N. F. Steinmetz, *Sci. Rep.* **2007**, *6*, 23803.

Manuscript received: January 21, 2022
Revised manuscript received: March 17, 2022
Accepted manuscript online: March 23, 2022
Version of record online: ■■, ■■■

RESEARCH ARTICLE

Biopanning led to the identification of tobacco mosaic virus (TMV)-binding peptides that can be utilized for diagnostic assays to detect TMV in plant sap or for biotechnology applications such as adding functional moieties to the TMV used as nanocarrier.

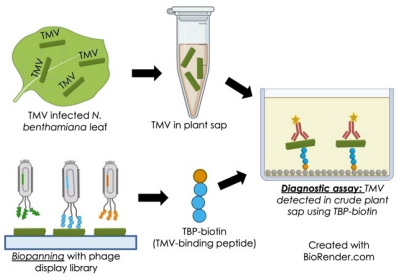

*Dr. S. K. Chan, Prof. Dr. N. F. Steinmetz**

1 – 8

Isolation of Tobacco Mosaic Virus-Binding Peptides for Biotechnology Applications